Numerical simulation and optimization on heat transfer and fluid flow in cooling channel of liquid rocket engine thrust chamber

Qiuwang Wang, Feng Wu, Min Zeng and Laiqin Luo
State Key Laboratory of Multiphase Flow in Power Engineering, Xi'an Jiaotong University, Xi'an, China, and
Jiguo Sun
Beijing Aviation Power Institute, China

Abstract

Purpose – To find the optimal number of channels of rocket engine thrust chamber, it was found that the optimal channel number is 335, at which the cooling effect of the thrust chamber cooling channel reaches the best, which can be helpful to design rocket engine thrust chamber.

Design/methodology/approach – The commercial computational fluid dynamics (CFD) software FLUENT with standard k-ε turbulent model was used. The CFD method was validated via comparing with the available experimental data.

Findings – It was found that both the highest temperature and the maximal heat flux through the wall on the hot-gas side occurs about the throat region at the symmetrical center of the cooling channel. Owing to the strong curvature of the cooling channel geometry, the secondary flow reached its strongest level around the throat region. The typical values of pressure drop and temperature difference between the inlet and exit of cooling channel were 2.7 MPa and 67.38 K (standard case), respectively. Besides an optimal number of channels exist, and it is approximately 335, which can make the effect of heat transfer of cooling channels best with acceptable pressure drop. As a whole, the present study gives some useful information to the thermal design of liquid rocket engine thrust chamber.

Research limitations/implications – More detailed computation and optimization should be performed for the fluid flow and heat transfer of cooling channel.

Practical implications – A very useful optimization on heat transfer and fluid flow in cooling channel of liquid rocket engine thrust chamber.

Originality/value – This paper provides the performance of optimization on heat transfer and fluid flow in cooling channel of liquid rocket engine thrust chamber, which can make the effect of heat transfer of cooling channels best with acceptable pressure drop. As a whole, the present study gives some useful information to the thermal design of liquid rocket engine thrust chamber.

Keywords Liquids, Rocket engines, Heat transfer, Gases, Optimization techniques

Paper type Research paper

Nomenclature

A = Local cross-sectional area, m^2
A_0 = Area of wall at hot-gas side, m^2
A_1 = area of base plane of ribs, m^2
A_2 = area of the extrude part of ribs, m^2

This work was supported by the NSFC Fund for Creative Research Groups (Grant No. 50521604) and Program for New Century Excellent Talents in University (Grant No. NCET-04-0938) of China.

Engineering Computations: International Journal for Computer-Aided Engineering and Software
Vol. 23 No. 8, 2006
pp. 907-921

0264-4401
DOI 10.1108/02644400610707793

A_t = cross-sectional area of throat, m^2
C^* = characteristic velocity, m s^{-1}
C_p = specific heat at constant pressure, kJ kg^{-1} K^{-1}
C_μ = constant in turbulence model
C_1 = constant in turbulence model
C_2 = constant in turbulence model
D_t = diameter at nozzle throat, m
h = convective heat transfer coefficient, W m^{-2}
h_{hyd} = convective heat transfer coefficient at gas-solid coupled interface, W m^{-2} K
h_{gas} = convective heat transfer coefficient at hot-gas side wall, W m^{-2} K
I = turbulence intensity, percent
k = ratio of specific heats; Turbulent kinetic energy, J m^{-3}
l = turbulent length scale, m
$\dot{m}$ = mass flow rate, kg/s
Ma = Mach number $= v/a$
M_r = relative molecular mass
n = normal outwardly with respect to solid wall
p_c^* = chamber pressure, Pa
P = pressure of hydrogen gas, MPa
P_{H_2O} = partial pressure of H_2O
P_{CO_2} = partial pressure of CO_2
Pr = Prandtl number $= \nu/\alpha$
q_r = radiative heat flux, W m^{-2}
q_w = wall heat flux, W m^{-2}
$q_{w,highest}$ = highest wall heat flux at hot gas side, W m^{-2}
S = source terms
T = temperature, K
T_{exit} = Outlet temperature of hydrogen gas, K
T_{gas} = hot gas static temperature, K
T_{hyd} = temperature of hydrogen gas, K
T_{in} = inlet temperature of hydrogen gas, K
T_w = wall temperature at gas side, K
$T_{w,highest}$ = highest wall temperature at hot gas side, K
T'_w = wall temperature of gas-solid coupled base surface, K
T^* = stagnation temperature, K
$\bar{T}_{hyd}$ = channel average temperature of hydrogen gas, K
u = velocity along x direction, m s^{-1}
u_{avg} = mean flow velocity of inlet, m s^{-1}
v = velocity along y direction, m s^{-1}
w = velocity along z direction, m s^{-1}
W = width of cooling channels, m
W_f = width of ribs in cooling channels, m
x = x axis of Cartesian Coordinate
y = y axis of Cartesian Coordinate
z = z axis of Cartesian Coordinate

Greek symbols
σ = dimensionless factor accounting for all corrections of property variation across boundary layer
σ_κ = turbulent Prandtl numbers for κ
σ_ε = turbulent Prandtl numbers for ε
σ_T = turbulent Prandtl numbers for T
ρ = density of hydrogen gas, kg m^{-3}
ϕ = general variable of conservation equations
η = viscosity, kg m^{-1} s^{-1}
η_t = turbulent viscosity, kg m^{-1} s^{-1}
η_{eff} = effective turbulent viscosity, kg m^{-1} s^{-1} ($= \eta + \eta_t$)
η_{hyd} = rib efficiency at hydrogen gas side
ε = dissipation rate of turbulent kinetic energy, m^2 s^{-3}
ε_g = emissivity of hot gas
ε_{H_2O} = emissivity of water vapour
ε_{CO_2} = emissivity of carbon dioxide
δ = thickness of wall, m
δT = local temperature difference between gas-solid coupled interface and hydrogen gas, K
λ = thermal conductivity of hydrogen gas, W K^{-1} m^{-1}
Γ_ϕ = diffuse coefficient
ΔT = inlet-outlet temperature difference for hydrogen gas, K

1. Introduction

The modern liquid rocket engine thrust chambers are exposed to high pressure and high temperature environments. The flow in the thrust chamber is turbulent and supersonic. In the H_2/O_2 liquid rocket engine, the flow and heat transfer of hydrogen gas in the cooling channel may be characterized as weakly compressible, high heat transfer rates, high Reynolds number turbulent flow and strong curvature effects in the cooling channel. Reducing wall temperature at hot-gas side wall by 50-100°C could result in the doubling of the chamber life cycle, which is very important to the industry of spaceflight due to the expensive cost of manufacturing. Therefore, how to enhance the cooling rate of thrust chamber is very important to the rocket engine.

Frohlich *et al.* (1991) and Lebail and Popp (1993) calculated the thermal performance of cooling channel, and owing to the limit of computer resource, only a parabolic marching numerical procedure was employed to calculate the flow and heat transfer in the rectangular cooling channels without re-circulation along the cooling channel. An integrated numerical models which incorporated computational fluid dynamics (CFD) for the hot-gas thermal environment, and thermal analysis for the liner and coolant channels, was developed by Wang and Luong (1992). Lai *et al.* (1994) proposed a concurrent processing approach for the coupling of multi-disciplinary analysis codes. Schmidt *et al.* (1998) has shown that the most efficient and straightforward design measure for increasing heat transfer of rocket chamber is decreasing of the hot gas wall surface temperature in the thrust chamber. Three concepts for enhancing heat transfer to the coolant have been selected and investigated experimentally by comprehensive subscale chamber hot-fire tests (Immich *et al.*, 2003): increasing the length of chamber cylinder, increasing the number of hot gas wall side ribs and artificially increasing the surface roughness. Heat transfer simulation and analysis of single geometrical parameter of liquid rocket cooling channel have been fulfilled, and the enhanced heat transfer by ribs has been reported in Immich *et al.* (1999, 2000). Li and Liu (2004) gained the temperature field in solid region of cooling channel using two-dimensional heat conduction model. Bucchi and Bruno (2005) investigated the heat transfer in the transpiration cooling performance in lox/methane liquid-fuel rocket engines, in which the real gas property was adopted. Wang and Luong (2004, 1994) studied on the cooling mechanism in liquid rocket engine. They concentrated on the methods of regenerative cooling and curtain cooling. They studied the hot-gas-side and coolant-side heat transfer in liquid rocket engine combustors using the holistic coupled model. In the liquid film cooling aspect, some experimental and analytical results have been reported in Kinney and Dukler (1952), Knuth (1953), William (1991) and Yan *et al.* (1991), but the details of transport process in the boundary layer have not been taken into account. Zhang *et al.* (2006) numerically studied the phenomena that characterize the exchange of heat and mass transfer between a hot gas stream and a thin liquid film in the two-dimensional model, in which the effects of gaseous radiation, external cooling and high temperature and high pressure of gases were all taken into account.

Three-dimensional analysis of heat transfer and fluid flow in a cooling channel of liquid rocket engine thrust chamber using gas-solid coupled technique was reported in Wu and Wang (2003) and Wu *et al.* (2005a, b). The computational results agreed well with the corresponding experimental results. To the authors' knowledge, the optimized calculation and analysis about cooling channel have not been reported. In this paper, the gas-solid coupled technique is adopted for seeking the optimal number of cooling channels for a liquid rocket engine thrust chamber. Figure 1 shows the thrust chamber of liquid rocket engine, for which totally 300 channels are used for cooling, and the total

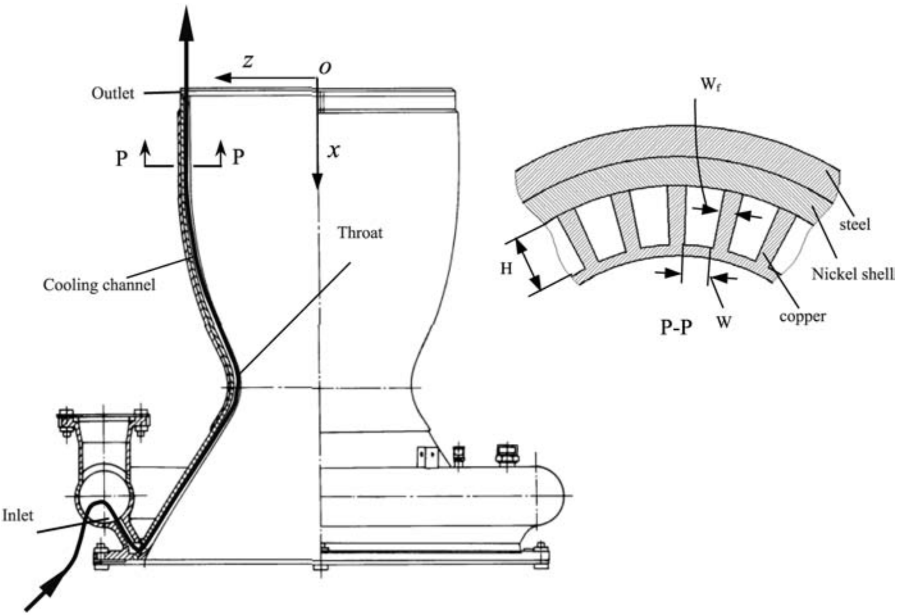

Figure 1.
Thrust chamber with cooling channel

mass flow-rate for 300 channels are 18.0 kg/s. The cooling channel is made up of copper, nickel shell and steel. The coolant is hydrogen gas with typical inlet temperature of 40 K and pressure of 15.2 MPa.

2. Mathematical description and numerical methods

2.1 Mathematical description

Figure 2 shows the cross-section of one cooling channel. As shown in the figure, the calculation may be carried out only for one-half of the channel because of the geometrical symmetry.

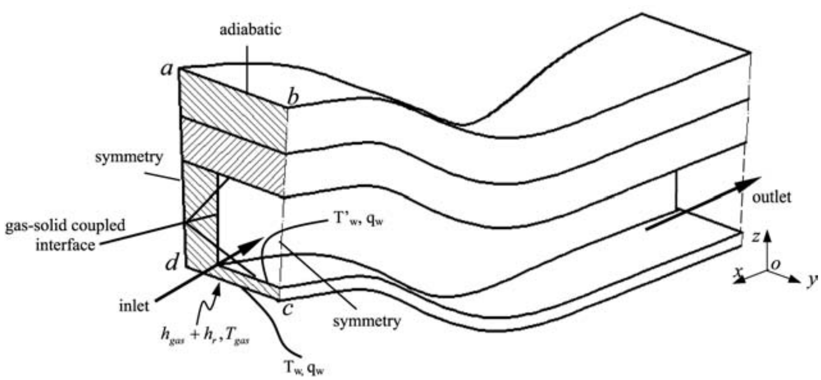

Figure 2.
Typical cooling channel cross-section

In the present work, the fluid flow and heat transfer in the cooling channel was assumed to be three-dimensional, steady-state and turbulent. The coolant (working fluid) is hydrogen gas. The conservation equations of fluid flow and heat transfer are expressed as (Tao, 2000):

$$\nabla \cdot (\rho \vec{V} \phi) = \nabla \cdot (\Gamma_\phi \nabla \phi) + S_\phi \tag{1}$$

where the expressions of ϕ, Γ_ϕ and S_ϕ for different variables can be found in Table I.

The standard k-ε two-equation turbulence model is employed to simulate the turbulent channel flow. Table II shows the corresponding values of constants in the turbulence model.

The convective heat transfer coefficient for the hot-gas side was calculated by the Bartz (1957) formula:

$$h_{\mathrm{gas}} = \frac{0.026}{d^{0.2}} \left(\frac{\eta^{0.2} C_{\mathrm{p}}}{Pr^{0.6}} \right) \left(\frac{p_{\mathrm{c}}^{*}}{C^{*}} \right)^{0.8} \left(\frac{A_{\mathrm{t}}}{A} \right)^{0.9} \sigma \tag{2}$$

The dimensionless factor, σ accounting for all corrections of property variation across boundary layer, was calculated by:

$$\sigma = \left[0.5 \frac{T_{\mathrm{w}}}{T^{*}} \left(1 + \frac{k-1}{2} Ma^2 \right) + 0.5 \right]^{-0.68} \left(1 + \frac{k-1}{2} Ma^2 \right)^{-0.12} \tag{3}$$

Prandtl number and viscosity η was approximately calculated by:

$$Pr \approx \frac{4k}{(9k-5)} \tag{4}$$

$$\eta \approx 1.184 \times 10^{-7} M_{\mathrm{r}}^{0.5} T^{0.6} \tag{5}$$

Equations	ϕ	Γ_ϕ	S_ϕ
Continuity equation	1	0	0
u equation	u	η_{eff}	$-\frac{\partial p}{\partial x} + \frac{\partial}{\partial x}\left(\eta_{\mathrm{eff}} \frac{\partial u}{\partial x}\right) + \frac{\partial}{\partial y}\left(\eta_{\mathrm{eff}} \frac{\partial v}{\partial x}\right) + \frac{\partial}{\partial z}\left(\eta_{\mathrm{eff}} \frac{\partial w}{\partial x}\right)$
v equation	v	η_{eff}	$-\frac{\partial p}{\partial y} + \frac{\partial}{\partial x}\left(\eta_{\mathrm{eff}} \frac{\partial u}{\partial y}\right) + \frac{\partial}{\partial y}\left(\eta_{\mathrm{eff}} \frac{\partial v}{\partial y}\right) + \frac{\partial}{\partial z}\left(\eta_{\mathrm{eff}} \frac{\partial w}{\partial y}\right)$
w equation	w	η_{eff}	$-\frac{\partial p}{\partial z} + \frac{\partial}{\partial x}\left(\eta_{\mathrm{eff}} \frac{\partial u}{\partial z}\right) + \frac{\partial}{\partial y}\left(\eta_{\mathrm{eff}} \frac{\partial v}{\partial z}\right) + \frac{\partial}{\partial z}\left(\eta_{\mathrm{eff}} \frac{\partial w}{\partial z}\right)$
Energy equation	T	$\eta/Pr + \eta/\sigma_T$	0
k equation	k	$\eta + (\eta_{\mathrm{t}}/\sigma_k)$	$\rho G_k - \rho\varepsilon$
ε equation	ε	$\eta + (\eta_{\mathrm{t}}/\sigma_\varepsilon)$	$\frac{\varepsilon}{k}(C_1 \rho G_k - C_2 \rho \varepsilon)$

Note: $G_k = (\eta_{\mathrm{t}}/\rho)[(\partial u/\partial x)^2 + (\partial v/\partial y)^2 + (\partial w/\partial z)^2] + ((\partial u/\partial y) + (\partial v/\partial x))^2 + ((\partial u/\partial z) + (\partial w/\partial x))^2 + ((\partial v/\partial z) + (\partial w/\partial y))^2$

Table I. Expressions of ϕ, Γ_ϕ and S_ϕ for different variables

C_μ	C_1	C_2	σ_k	σ_ε	σ_T
0.09	1.44	1.92	1.0	1.3	0.85

Table II. Constants in k-ε turbulence model

The radiation heat transfer of hot-gas side was calculated by:

$$q_{\mathrm{r}} = \varepsilon_{\mathrm{g}}\sigma\left(T_{\mathrm{gas}}^{4} - T_{\mathrm{w}}^{4}\right) \tag{6}$$

where T_{gas} is the temperature of hot gas, T_{w} is the wall temperature of hot-gas side, ε_{g} is the effective emissivity of hot gas.

2.2 Numerical methods and boundary conditions

The numerical simulation work was carried out by the commercial software FLUENT and the grid system was built in GAMBIT. The numerical method for solving the governing equations was based on the conservation finite-volume method. The *Re* number of computational rocket engine cooling channel reaches 7.6×10^5. In references Takase (1996) and Choi and Anand (1995), the standard k-ε two-equation model has been used to simulate turbulent heat transfer with high Reynolds ($Re = 300$-$60{,}000$) number in a limited channel, and the numerical results agreed well with the experimental data. Thus, in this paper the standard k-ε two-equation turbulence model was also employed. The SIMPLER algorithm was used to solve the pressure-velocity coupled equations. The QUICK scheme was used for convection terms in the governing equations. Standard wall function method was adopted for the near-wall treatment. The first grid node away from the wall was placed at the non-dimensional distance $y_p^+ = 30 \sim 300$. The total number of grid points in the calculation domain was $300(\mathrm{x}) \times 40(\mathrm{y}) \times 60(\mathrm{z})$, which was fine enough to obtain grid-independent results.

The boundary conditions of computational domain are described as shown in Figure 2.

At inlet:

$$\text{fluid region}: \dot{m} = 0.03\,\mathrm{kg/s},\quad T = 40\,\mathrm{K},\quad P = 15.2\,\mathrm{MPa}\,\text{(typical case)} \tag{7a}$$

$$k = 1.5(u_{\mathrm{avg}}I)^2,\quad \varepsilon = C_\mu^{3/4}\frac{k^{3/2}}{l} \tag{7b}$$

$$\text{solid region}: \frac{\partial T}{\partial x} = 0,\quad u = v = w = 0 \tag{7c}$$

At outlet:

$$\text{fluid region}: \frac{\partial u}{\partial x} = \frac{\partial v}{\partial x} = \frac{\partial w}{\partial x} = \frac{\partial T}{\partial x} = \frac{\partial k}{\partial x} = \frac{\partial \varepsilon}{\partial x} = 0 \tag{7d}$$

$$\text{solid region}: \frac{\partial T}{\partial x} = 0,\quad u = v = w = k = \varepsilon = 0 \tag{7e}$$

$$\text{boundary } ab: \frac{\partial T}{\partial z} = 0,\quad u = v = w = k = \varepsilon = 0 \tag{7f}$$

Boundary *bc*:

$$\text{fluid region}: \frac{\partial u}{\partial y} = \frac{\partial w}{\partial y} = \frac{\partial T}{\partial y} = \frac{\partial k}{\partial y} = \frac{\partial \varepsilon}{\partial y} = 0,\quad v = 0 \tag{7g}$$

$$\text{solid region}: \frac{\partial T}{\partial y} = 0, \quad u = v = w = k = \varepsilon = 0 \tag{7h}$$

$$\text{Boundary } ad: \frac{\partial T}{\partial y} = 0, \quad u = 0, v = w = k = \varepsilon = 0 \tag{7i}$$

$$\text{Boundary } cd: (h_{\text{gas}} + h_{\text{r}})(T_{\text{w}} - T_{\text{gas}}) = -\lambda\left(\frac{cT}{\partial n}\right)_{\text{wall}}. \tag{7j}$$

Equation (7j) is a heat balance at the boundary between hot gas and solid wall, λ is the thermal conductivity of solid wall, n is an outward normal coordinate and $(\partial T/\partial n)_{\text{wall}}$ is temperature gradient indicating solid wall normal to the outward. h_{gas} is the convective heat transfer coefficient, determined by Bartz formula (equation (2)), and h_{r} is the radiative heat transfer coefficient, determined by:

$$h_{\text{r}} = \frac{q_{\text{r}}}{T_{\text{w}} - T_{\text{gas}}} = \frac{\varepsilon_{\text{g}}\sigma\left(T_{\text{w}}^4 - T_{\text{gas}}^4\right)}{T_{\text{w}} - T_{\text{gas}}} \tag{7k}$$

Hot gas emissivity ε_{g} is calculated by the equation $\varepsilon_{\text{g}} = \varepsilon_{H_2O} + \varepsilon_{CO_2} - \varepsilon_{H_2O}\cdot\varepsilon_{CO_2}$, ε_{H_2O} and ε_{CO_2} are determinated by partial pressure p_{H_2O}, p_{CO_2} and hot gas static temperature T_{g}, which can be found in Feng and Zhang (1991). The gas emissivity has little influence on the heat transfer in rocket engine thrust chamber when it varies within small range. According to the conditions of this study, the emissivity ε_{g} is about 0.45.

3. Results and discussion

3.1 Validation of numerical model

The standard $k \sim \varepsilon$ turbulence model and large eddy simulation (LES) were used to simulate temperature and velocity distribution in fluid and solid region of the regenerative-cooling channel in order to test and validate the calculation method and model (Wu *et al.*, 2005a). The Smagorinsky-Lilly subgrid scale model was used, which is the most basic of subgrid-scale models proposed by Smagorinsky and further developed by Smagorinsky (1963), Lilly (1966) and Yuu *et al.* (2001). The simulation results of the two turbulence models are compared with the experimental data at different calculation grids (Table III). It is shown that under the same grids, the results obtained by standard $k \sim \varepsilon$ turbulence model agreed better with the experimental data than those by LES. The deviations of inlet-outlet temperature difference and inlet-outlet pressure drop were 4.3 and 12.5 percent between numerical results by $k \sim \varepsilon$ model and experimental data, respectively. With the increase of calculation grids, the calculation precision of LES was gradually enhanced. In this paper, the standard $k \sim \varepsilon$ turbulence model was adopted to simulate and optimize the heat transfer and flow of liquid rocket engine chamber.

3.2 Numerical analysis of a standard case

The above procedure was first applied to predict the turbulent flow and heat transfer in a typical cooling channel of a rocket engine thrust chamber (Figure 1). In the present calculation, the roughness of copper surface was assumed to be 6.5 μm, while it was 50 μm for nickel surface. The cross-section average temperature and heat flux

Table III.
Comparisons of results among experimental data, $k \sim \varepsilon$ model and LES model under different grids

	Temperature difference between inlet and outlet of hydrogen gas (K)			Pressure drop between inlet and outlet of hydrogen gas (MPa)		
Turbulence models/experimental data	$285 \times 12 \times 30$	$300 \times 20 \times 40$	$300 \times 30 \times 45$	$285 \times 12 \times 30$	$300 \times 20 \times 40$	$300 \times 30 \times 45$
LES	96.5	97.7	102.2	0.06	0.10	0.138
k-ε	106.3	106.3	106.5	0.35	0.35	0.352
Experimental data		110			0.4	

distributions in the wall on the hot gas side along the flow direction are shown in Figure 3, which indicates that the highest wall temperature (545.9 K) on the hot gas side occurred at the throat region ($x = 0.38$ m). The melting point temperature of copper is 900 K (Feng and Zhang, 1991), so it indicates that the copper was within the safe range. On the other hand, the maximal heat flux (6.34×10^7 W/m^2) imposed to the wall on the hot gas side also occurred at the throat region. The pressure drop and temperature difference between the inlet and the exit of the cooling channel are 2.7 MPa and 67.38 K, respectively. It may be seen that the copper wall of the throat region in the hot gas side must endure the highest temperature and maximal heat flux, so this region should be taken into special account during the thermal design of thrust chamber.

Variations of average hydrogen gas temperature in a cooling channel and average convective heat transfer coefficient at a gas-solid coupled interface are shown in Figure 4. Variations of average wall temperature and heat flux at a gas-solid coupled interface are shown in Figure 5. It indicates that maximal heat flux and maximal convective heat transfer coefficient simultaneously occur at the throat region of rocket

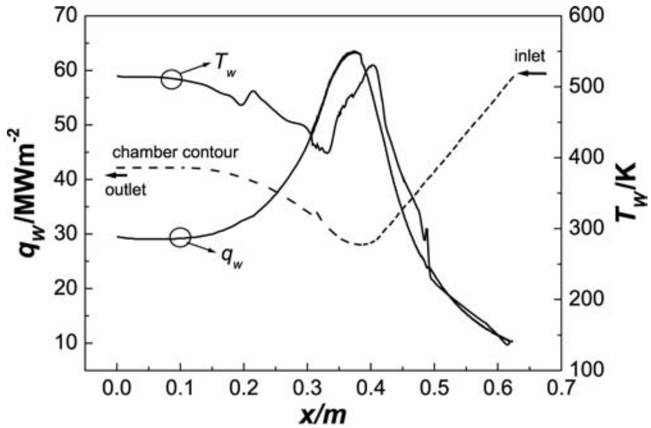

Figure 3.
Variations of wall temperature T_w and heat flux q_w at the hot-gas side

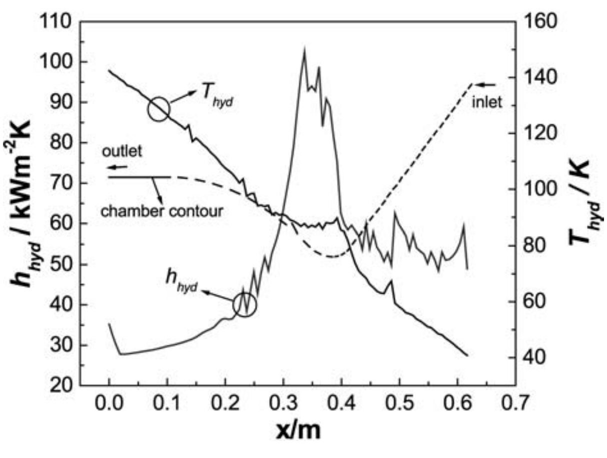

Figure 4.
Variations of average temperature of hydrogen gas T_{hyd} in cooling channel and average convective heat transfer coefficient h_{hyd} at gas-solid coupled interface

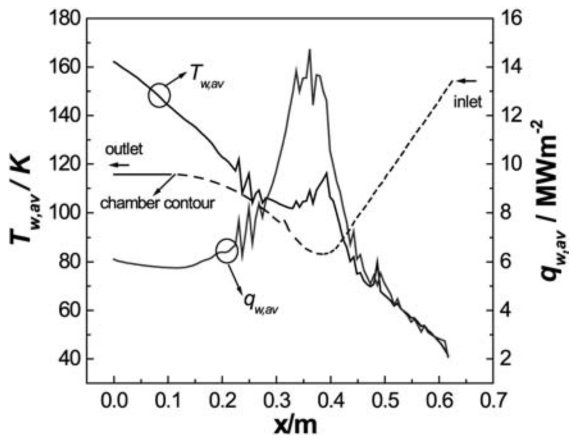

Figure 5.
Variations of average wall temperature and heat flux at gas-solid coupled interface

thrust chamber because the velocity of hydrogen gas V reaches the maximum value near the throat region (Figure 6), whose cross-sectional area is minimum. Figure 6 also shows the local distribution of temperature difference δT between the gas-solid coupled interface and hydrogen gas.

Figures 7 and 8 show the temperature contours and velocity distributions in different regions (inlet, outlet and throat) along the x coordinate. It can be seen from these figures the temperature distribution in the cross-section at the throat region is higher than those at the other two cross-sections. The highest temperature in the cross section occurred at point c and the maximal heat flux occurred at point d of the copper wall on the hot-gas side (Figure 2). This is because the heat conduction effect of the copper ribs at point d enhances the heat transfer of the cooling channels.

3.3 Optimization simulation

The thrust chamber liner is made from copper, with axial slots milled into this copper body. Recent experimental study on the high-aspect-ratio cooling passages demonstrated that a large number of cooling passages increase the potential for

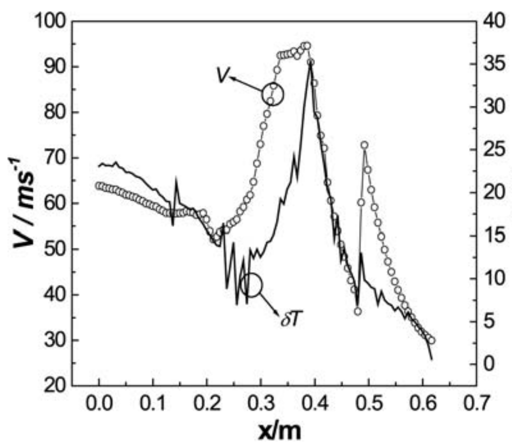

Figure 6.
Variations of average velocity V and temperature difference δT between gas-solid coupled interface and hydrogen gas

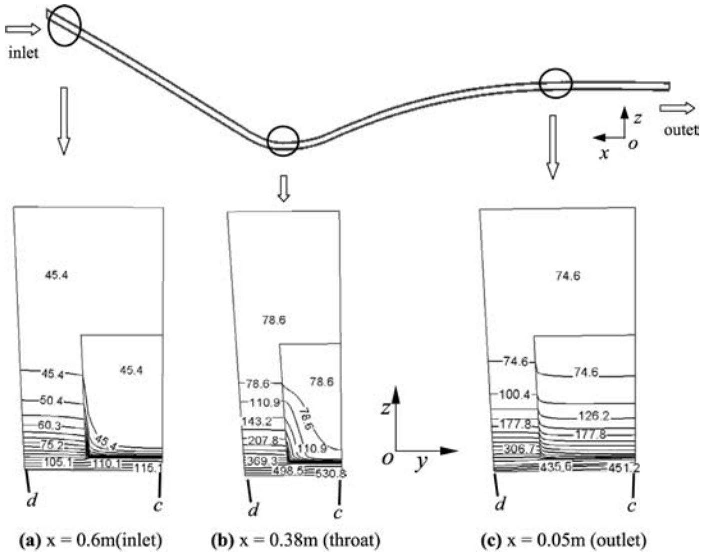

Figure 7.
Temperature distribution of cooling channel in different regions (not to scale)

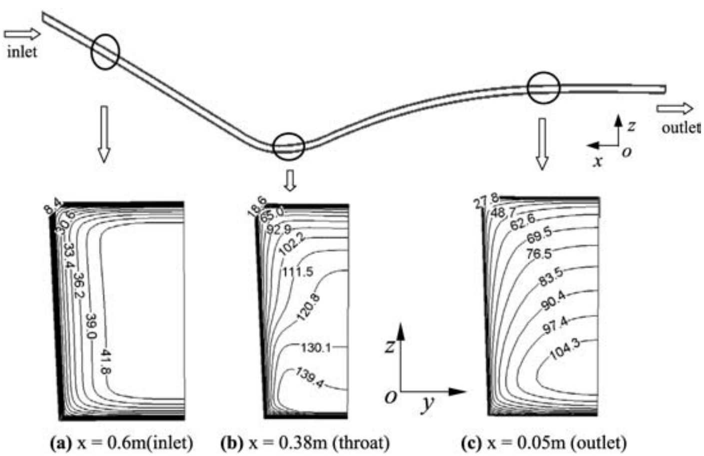

Figure 8.
Velocity distribution of cooling channel at different regions (not to scale)

longer life than fewer channels under given thrust chamber dimensions. More channels results in larger aspect ratios in the channel cross-section (Lebail and Popp, 1993). In order to improve heat transfer rate of rocket cooling channels, an optimization calculation was performed to find out the optimal number of cooling channels. Under the same boundary conditions and keeping the height of channel and width of the fins as constants, when the number of cooling channels was changed, the width of channels and the mass flow-rate of hydrogen gas in the single cooling channel were changed.

By changing the number of the cooling channels, the heat transfer characteristics of cooling channels were changed consequently. Variations of highest wall temperature T_{w} and average heat flux q_{av} of the wall in the hot-gas side versus the number of the cooling channels are shown in Figure 9. The variations of pressure drop ΔP and the temperature difference ΔT between the inlet and exit of cooling channels coolant are shown in Figure 10.

Figures 9 and 10 show that there exists an optimal number of cooling channels (about 335), which has highest wall heat flux (about 31 MW/m^2) at hot gas side wall and highest temperature difference (about 76 K) between inlet and outlet, and lowest wall temperature (about 550 K) at hot gas wall, while the pressure drop between inlet and outlet is not so high (about 1.3 MPa) and may be acceptable from the engineering point of view.

This phenomenon could be explained as follows. The average temperature of hydrogen gas in the cooling channels can be defined as the average value of the inlet and exit gas temperature:

$$\bar{T}_{\mathrm{hyd}} = \frac{(T_{\mathrm{in}} + T_{\mathrm{exit}})}{2} \tag{8}$$

The values calculated for different numbers of channels are displayed in Table IV.

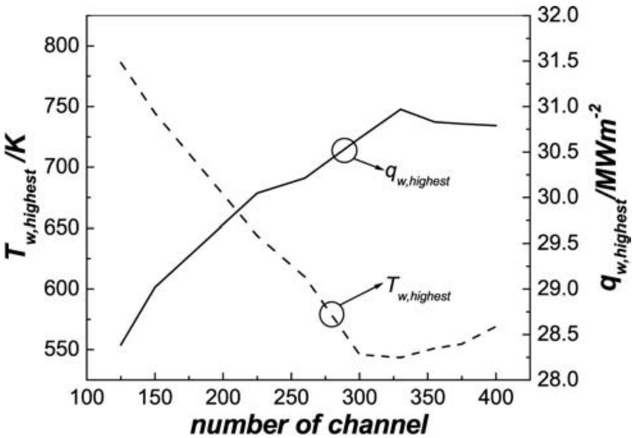

Figure 9.
Variations of highest temperature and wall highest heat flux at hot-gas side wall

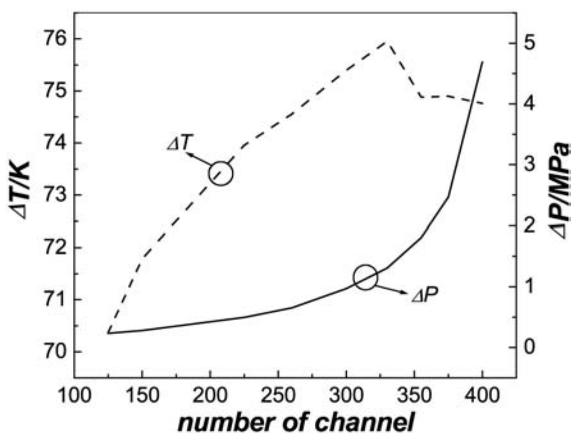

Figure 10.
Variations of temperature difference and pressure drop between inlet and outlet of cooling channel

It can be seen from Table IV that the average temperature of hydrogen gas almost keeps constant. Figure 11 shows the heat transfer resistance sketch map of cooling channels. We may assume that $1/[(h_{\mathrm{hyd}} + h_{\mathrm{r}})A_0]$ and $\delta/(\lambda A_0)$ (Figure 11) keep constant when the average temperature of hot gas (T_{gas}) and hydrogen gas (T_{hyd}) keep constant. With the increase of the number of cooling channels, the velocity of hydrogen gas will increase, so both the convective heat transfer coefficient of hydrogen gas in cooling channels, h_{hyd}, and the fin area A_2, will increase. On the other hand, both the base area A_1 and rib efficiency η_{hyd} will decrease. As a result, there exists an optimal number of channels which leads $(A_1 + A_2\eta_{\mathrm{hyd}})h_{\mathrm{hyd}}$ to achieve maximum value, and hence the temperature of the wall in the hot-gas side (T_{w} in Figure 11) comes to its minimum, and the corresponding heat flux at hot-gas side wall reaches the maximum (Figure 9). It should be noted that for thrust chamber for liquid rocket engine, having the highest wall heat flux at side wall with the smallest penalty of pressure drop is the most important for thermal design of rocket engine thrust chamber.

Table IV. $\bar{T}_{\mathrm{hyd}}$ for different numbers of channels

N	125	150	225	330	355	375
$\bar{T}_{\mathrm{hyd}}$(K)	82.0	82.48	82.59	83.3	82.8	82.6

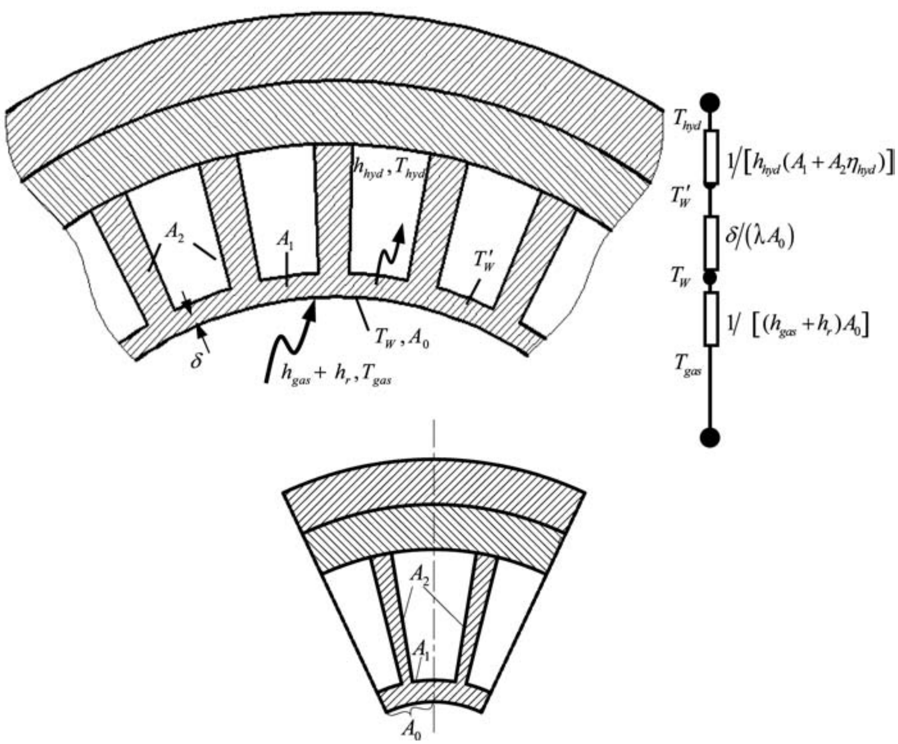

Figure 11. Heat transfer resistance sketch map of cooling channel

4. Conclusions

A three-dimensional gas-solid coupling solution program was employed to calculate the flow and heat transfer in cooling channels of thrust chamber with high aspect ratio. The numerical method was validated by comparing the calculated results with previous experimental data. It indicates that both the highest temperature and the maximal heat flux through the wall on the hot-gas side occurs about the throat region at the symmetrical center of the cooling channel. Owing to the strong curvature of the cooling channel geometry, the secondary flow reached its strongest level around the throat region. The typical values of pressure drop and temperature difference between the inlet and exit of cooling channel were 2.7 MPa and 67.38 K (standard case), respectively.

Based on the calculation and analysis of heat transfer character of the cooling channels by changing number of cooling channels and keeping boundary conditions constant, it was found that an optimal number of channel exists, and it is approximately 335, which can make the effect of heat transfer of cooling channels best with acceptable pressure drop. As a whole, the present study gives some useful information to the thermal design of liquid rocket engine thrust chamber.

References

Bartz, D.R. (1957), "A simple equation for rapid estimation of rocket nozzle convective heat transfer coefficients", *Jet Propulsion*, Vol. 27 No. 1, pp. 49-51.

Bucchi, A. and Bruno, C. (2005), "Congiunti cooling performance in lox/methane liquid-fuel rocket engines Bucchi, Andrea", *Journal of Spacecraft and Rockets*, Vol. 42 No. 3, pp. 476-86.

Choi, J.M. and Anand, N.K. (1995), "Turbulent heat transfer in a serpentine channel with a series of right-angle turns", *International Journal of Heat and Mass Transfer*, Vol. 38 No. 7, pp. 1225-36.

Feng, W.L. and Zhang, Y.J. (1991), *Theory of Liquid Rocket Engine*, BeiHang University Press, BeiJing (in Chinese).

Frohlich, A., Immich, H., Lebail, F., Popp, M. and Scheuerer, G. (1991), "Three-dimensional flow analysis in a rocket engine coolant channel of high depth/width ratio", AIAA Paper 91-2183.

Immich, H., Alting, J., Kretschmer, J. and Preclik, D. (2003), "Technology development for thrust chambers of future launch vehicle liquid rocket engines", *Acta Astronayica*, Vol. 53, pp. 597-605.

Immich, H., Frohlich, T. and Kretschmer, J. (1999), "Technology developments for expander cycle engine thrust chambers", AIAA Paper, 35th Joint Propulsion Conference, Los Angeles, CA.

Immich, H., Kretschmer, J. and Preclik, D. (2000), "Technology developments for cryogenic rocket engines", AIAA Paper, 2000-3780. 35th Joint Propulsion Conference. Huntscille, AL.

Kinney, G.R. and Dukler, A.E. (1952), "Internal liquid film cooling experiments with air stream temperatures to 2000F in 2- and 4-inch diameter horizontal tubes", NACA Report.

Knuth, E.L. (1953), "The mechanics of film cooling", *JPL Memo*, September, pp. 20-85.

Lai, Y.G., Przekwas, A.J. and Nguyen, N. (1994), "A concurrent multi-disciplinary approach for the analysis of liquid rocket engine combustors", AIAA Paper 94-3103.

Lebail, F. and Popp, M. (1993), "Numerical analysis of high aspect ratio cooling passage flow and heat transfer", AIAA Paper 93-1829.

Li, J.W. and Liu, Y. (2004), "Method of computing temperature field in regeneration-cooled thrust chamber", *Journal of Aerospace Power*, Vol. 19 No. 4, pp. 550-6.

Lilly, D.K. (1966), "On the application of the eddy viscosity concept in the inertial subrange of turbulence", NCAR Manuscript 123, National Center for Atmospheric Research, Boulder, CO.

Schmidt, G., Popp, M. and Frohich, Th. (1998), "Design studies for an 10 ton class high performance expander cycle engine", AIAA Paper 98-3673.

Smagorinsky, J. (1963), "General circulation experiments with the primitive equations I", *The Basic Experiment. Month. Wea. Rev.*, Vol. 91, pp. 9-164.

Takase, K. (1996), "Numerical prediction of augmented turbulent heat transfer in an annular fuel channel with repeated two-dimensional square ribs", *Nuclear Engineering and Design*, Vol. 165 Nos 1/2, pp. 225-37.

Tao, W.Q. (2000), *Numerical Heat Transfer*, 2nd ed., Xi'an Jiaotong University Press, Xi'an (in Chinese).

Wang, T.S. and Luong, V. (1992), "Numerical analysis of the hot-gas-side and coolant-side heat transfer for liquid rocket engine combustors", AIAA Paper 92-3151.

Wang, T.S. and Luong, V. (1994), "Hot-gas-side and coolant-side heat transfer in liquid rocket engine combustors", *Journal of Thermophysics and Heat Transfer*, Vol. 8 No. 3, pp. 524-30.

Wang, T.S. and Luong, V. (2004), "Numerical a study on the cooling mechanism in liquid rocket engine", paper presented at 40th AIAA/ASME/SAE/ASEE Joint Propulsion Conference and Exhibit; Fort Lauderdale, FL, July, pp. 11-4.

William, M.G. (1991), "Liquid film cooling in rocket egines", CD Report, March.

Wu, F. and Wang, Q.W. (2003), "Numerical simulation on heat transfer and fluid flow in cooling channel of liquid rocket engine thrust chamber", paper presented at the 16th Conference of Calculation Mechanics, Mechanical Institute of Japan, pp. 177-8.

Wu, F., Wang, Q.W., Luo, L.Q. and Sun, J.G. (2005a), "Numerical investigation of turbulent models on heat transfer and fluid flow in cooling channel of H2/O2 liquid rocket engine thrust chamber", *Journal of Propulsion Technology*, Vol. 26 No. 5, pp. 389-93.

Wu, F., Wang, Q.W., Luo, L.Q. and Sun, J.G. (2005b), "Numerical simulation on heat transfer and fluid flow in cooling channel of liquid propellant rocket engine thrust chamber", *Journal of Aerospace Power*, Vol. 20 No. 4, pp. 197-202.

Yan, W.M., Lin, T.F. and Tsay, Y.L. (1991), "Evaporative cooling of liquid film through interfacial heat and mass transfer in a vertical channel: I-experimental study", *International Journal of Heat and Mass Transfer*, Vol. 34, pp. 1105-11.

Yuu, S., Ueno, T. and Umekage, T. (2001), "Numerical simulation of the high Reynolds number slit nozzle gas-particle jet using subgrid-scale coupling large eddy simulation", *Chemical Engineering Science*, Vol. 56 No. 14, pp. 4293-307.

Zhang, H.W., Tao, W.Q., He, Y.L. and Zhang, W. (2006), "Numerical study of liquid film cooling in a rocket combustion chamber", *International Journal of Heat and Mass Transfer*, Vol. 49, pp. 349-58.

Corresponding author
Qiuwang Wang can be contacted at: wangqw@mail.xjtu.edu.cn